Al-Rafidain Journal of Engineering Sciences

Journal homepage https://rjes.iq/index.php/rjes

ISSN 3005-3153 (Online)

AI-Enabled IoT-Based Smart Grid Fault Detection and Load Optimization for Renewable Energy Integration

Ammar Jalal Abdulrazzaq Al-Tabatabaee

Assistant Governor for Technical Affairs, Wasit Province, Iraq

ARTICLE INFO

Article history:
Received 19 December 2025
Revised 19 December 2025,
Accepted 01 January 2026,
Available online 03 January 2026

Keywords:
AI-enabled smart grid
Internet of Things (IoT)
Fault detection
Load optimization
Renewable energy integration

ABSTRACT

Rising penetration of renewable energy sources presents significant challenges to smart grid operations, especially in fault detection, power quality, and cost-effective energy management. In this research, suggest a smart grid framework with AI-supported IoT that combines real-time fault detection solution and intelligent load monitoring for the smart grid for grid reliability and the renewable energy supply optimization. Electrical and environmental information such as voltage, current, frequency, total harmonic distortion, power quantities, power factor, and temperature are gathered by IoT sensors and processed through an efficient, toolbox-free AI-powered, computationally efficient artificial intelligence model. A custom multi-class K-Nearest Neighbors classifier is applied in fault detection with a high sensitivity classification accuracy score of 97.67%, perfect detection accuracy for harmonic and overcurrent failures and strong classification results for voltage sag, swell and frequency deviation events. Concurrently, a mixed-integer linear programming–based optimization approach is proposed to plan flexible load utilization and reduce the energy requirement associated with grid use in an environment with time-varying tariffs and renewable resources. The optimization results indicate that about 700 kWh of renewable energy is used effectively as opposed to 490 kWh of grid-imported energy, yet renewable energy curtailment is below 1%, indicating that demand–supply is good coordination. At the same time, a fault-aware optimization framework drastically reduces the total operational cost and renewable energy waste and grid dependency, while guaranteeing high reliability in fault detection. The solutions demonstrate that the method proposed is suitable for real-time rollout in intelligent, reliable, and sustainable smart grid systems.

1. Introduction

The explosive development of renewables, including solar and wind power, has greatly expanded the shape and process of the current electrical power networks. Despite promoting sustainability and emission reduction, high integration of renewable power sources generates challenges connected with power quality, system reliability, and operational efficiency. The variability and irregularity in renewable generation, combined with the increasing complexity of the distributed load, result in the inability of traditional monitoring and control methods for the smart grid of today. In this regard, Internet of Things (IoT) and its technologies enable continuous real-time monitoring of electrical and environmental parameters across power networks. IoT sensors measure voltage, current, frequency, harmonic distortion, power flow, and temperature in high-resolution, forming the basis of data-driven smart grid functioning. But large quantities of data don't solve grid performance issues on their own without intelligent analysis and decision-making mechanisms. Artificial intelligence (AI) has proved out to be a strong method for studying complex and nonlinear behaviour of smart grid data, especially in fault detection and power quality determination. Artificial intelligence based models showed higher accuracy in abnormal operating conditions detection than traditional threshold detection

Corresponding author E-mail address: ammar.jalal1975@gmail.com
https://doi.org/10.61268/6j5zpx37

methods. However, most of the published literature have primarily been based on fault detection and have not considered how these can be incorporated into energy management and load scheduling, which limits their applicability in live grid operation where fault and operation decisions are closely linked to each other.

(Adefarati et al., 2025) [1] detailed a thorough review discussing how IoT and AI contribute to improving the monitoring, control and reliability of renewable-dominant power systems. Their research highlighted AI-driven forecasting and real-time optimization as driving factors of high renewable penetration. (Alijoyo, 2024) [2] explored deep learning-based energy management frameworks for Industry 4.0 smart buildings. Results showed major gains in energy efficiency based on predictive control and adaptive demand-side management. (Areola et al., 2025) [3] critically reviewed AI techniques for optimizing solar power systems integrated with energy storage. The authors highlighted trends, pointing to future directions but also presented problems in data quality, scalability, and system interoperability. (Arévalo & Jurado, 2024) [4] used AI to understand the design and operation of distributed energy systems in smart grids. Their findings revealed how AI enhances dispatch decisions, system flexibility and operational resilience. (Awad & Bayoumi, 2025) [5] described an integrated AI & cybersecurity/regulatory perspective of next-generation smart inverters by incorporating AI, cybersecurity and regulatory aspects. The research emphasized the significance of intelligent inverters as providing grid stability during the energy transition. (Bajahzar, 2024) [6] investigated the AI-based Internet of Everything services for the smart home. According to the study, the intelligent automation has the positive impacts of increasing user comfort, saving energy and responding to the system. (Bajwa et al., 2025) [7] performed a systematic literature review on AI-powered smart building management systems. Their findings validated significant reductions in energy consumption and emissions via AI-centered optimization strategies. (Benson & Eronu, 2025) [8] evaluated the combination of thermal-based power systems with renewable electricity. The research highlighted the importance of optimization and storage mechanisms to sustain the reliability of the grid in response to fluctuating amount of renewable energy. (Das, 2025) [9] investigated the relationship between IoT and AI for sustainable and energy efficient smart buildings. The paper also found some technical obstacles and recommended strategic directions for large-scale deployments. (Goudarzi et al., 2022) [10] surveyed smart grid technologies supporting IoT, which includes architecture, application, and obstacles. Thus they established a basic overview of communication, data analytics and security issues. (Ifeanyi Kingsley et al., 2025) [11] explored the latest developments in AI driven energy management systems for renewable integrated smart grids. A study of the effectiveness of AI in demand forecasting and optimization of energy dispatch was identified in the study. (Ikegwu et al., 2025) [12] explored the potential of AI and machine learning in monitoring and optimizing energy consumption in smart homes. Their findings indicated greater accuracy in predicting consumption and fault detection. (Joshua et al., 2024) [13] introduced a hybrid machine learning model for solar energy potential analysis and fault detection in AIoT-based solar–hydrogen power plant. The framework improved system reliability and predictive capability. (Karim et al., 2025) [14] presented a preprint study focusing specifically on newly deployed AI-driven methodology for energy systems analysis. The report highlighted future research avenues of intelligent energy optimization. (Mahmud & Waheduzzaman, 2025) [15] studied the contribution of artificial intelligence in smart grid technologies in smart system design. The research drew attention to AI's role in predicting load, diagnosis of faults and also of grid automation. (Mawat & Hamdan, 2023) [16] described hydrodynamic and water quality modeling methods, which were applied for surface water environment. Their research contributed knowledge useful in the environmental monitoring and sustainable

resources management. (Nuruzzaman et al., 2025) [17] performed a systematic review on predictive maintenance for power transformers based on AI and IoT. Through diagnostics driven by data, the findings suggested reduced downtime and improved life for assets. (Nuruzzaman & Rana, 2025) [18] focused on IoT-enabled condition monitoring for power distribution systems. This study focuses on SCADA integration, real-time analytics and overcoming cyber-physical security issues. (Nuthakki et al., 2022) [19] studied the benefits to the company with AI-enabled smart meters in enhancing customer satisfaction. They found that they improved billing accuracy, demand awareness, and energy management. (Ojadi et al., 2024) [20] for energy efficiency and reducing carbon footprint, they examine AI-enabled smart grid systems for urban networks. The findings validated AI's role in sustainable urban energy planning. (Rana, 2025) [21] examined AI-driven fault detection and predictive maintenance of power systems. Digital twins and self-healing grid concepts were integrated into the study. (Rojek et al., 2025) [22] has shown that a case study about use of IoT and AI-based applications of IoT to save energy in buildings has been delivered using the case example of how to integrate IoT and AI applications for building energy management. The findings showed good real-time optimization on time, energy consumption optimization and reduction in consumption of energy use were well presented with an effective effect of the results. (Sankarananth et al., 2023) [23] proposed AI-enabling metaheuristic optimization strategies for predictive management of renewable energy production. Their method led to enhanced predictions and an increase of grid efficiency. (Sarin et al., 2025) [24] performed a bibliometric-supported systematic literature search for AI-based renewable microgrid optimization. This study noted some research gaps and discussed future directions regarding intelligent microgrids. (Stecuła et al., 2023) [25] studied AI powered urban energy solutions from a local to societal scale. The report highlighted the role of AI in realizing smart, low-carbon cities. (Udoka Eze, 2025) [26] proposed AI-based MPPT model on hybrid solar–wind systems for off-grid rural electrification. The results indicated increased efficiency of energy harvesting and reliability of the system. (Ukoba et al., 2024) [27] overviewed AI use cases in refining renewable energy systems. Future outlook for intelligent control, forecasting, and system integration was provided by the study.

Despite the increasing literature on AI and IoT-enabled smart grid applications within a wide range of smart grid fields, a number of important gaps persist in current research. Most previous researches have treated fault detection, renewables management and load optimization as independent issues and not taking into account the high coexistence of the issues in everyday smart grid. AI-driven fault detection strategies in particular tend to be developed as independent monitoring devices and are not incorporated into real-time energy management or load scheduling decision-making. Likewise, load optimization studies commonly assume the presence of ideal grid conditions, ignoring the influence of the power quality irregularities and faults on operational tactics. The recent contribution of this paper is the proposed unified AI-based IoT-based smart grid system that combines multi-class fault detection and load optimization under renewable energy integration. Contrasting to previous methods, this research connects the real-time fault classification prediction results and operational load scheduling to realize dynamic, energy-aware fault-analysis. More importantly, this method combines electrical, power quality and thermal features and provides a single AI model's complete data that allows a holistic physical representation of the grid behaviour. Furthermore, an AI implementation is computationally efficient and toolbox-free with a mixed-integer optimization formulation that increases practical deployability in real-time and resource-constrained environments. The proposed framework will push the smart grid through to operate more reliably, sustainably, and even high-smart autonomous systems by addressing these gaps.

2. Methodology

2.1 System overview

Thus, the proposed system is an AI-enabled IoT-based smart grid framework, which will bring reliable fault detection and cost-efficient load optimization during a high renewable penetration condition. This is a unified architecture consisting of distributed IoT sensors, an artificial intelligence decision layer, and an energy management module. It collects electrical and environmental measures in near real-time (voltage, current, frequency, total harmonic distortion, power quantities, temperature) continuously from core grid nodes and sends it to a central processing unit. At the analytical level, the obtained data is preprocessed and presented to an AI-based fault detection model which classifies the grid operating state as normal or specific fault conditions. Simultaneously, a load and renewable energy modeling module predicts available solar and wind generation, in addition to flexible load capacities. Using these inputs, an optimization module will schedule controllable loads in a way which allows for the minimization of energy cost, while operating to satisfy fixed operational constraints and maintaining the strength of the grid stability. Fault detection/load optimization interaction provides the opportunity for adaptive and robust operation of the grid from an adaptive dynamic system to be able to dynamically respond to disturbances and renewable variability. Indeed, the presented framework offers a scalable and computationally effective approach to intelligent monitoring and energy management in the context of contemporary smart grids.

2.2 Data and fault modelling

Here, apply a synthetic IoT dataset to model the smart grid operating data that represents normal and failing electrical & environmental behavior. A total of 6000 samples are generated, of which 80% (4800 samples) are for normal operating conditions and 20% (1200 samples) are for fault scenarios. The eight measured features of each sample are:

- Voltage magnitude (V_{pu}),
- Current magnitude (I_{pu}),
- Grid frequency (f_{Hz}),
- Total harmonic distortion (THD%),
- Active power (P_kW),
- Reactive power (Q_kVAr),
- Power factor (PF),
- Temperature ($Temp_C$).

In normal operation, normal values are near nominal values like a voltage mean of about 0.996 p.u., frequency around 50.0 Hz, THD around 2%, and temperature of 35.7 °C suggesting steady state grid performance. To implement physically meaningful deviations from the nominal values, fault conditions are modeled. Voltage sag faults are described by a voltage of no less than 0.75 p.u., and voltage swell faults represent a voltage of up to 1.21 p.u.. Frequency deviation issues bring oscillations of 48.35 Hz−51.72 Hz, which indicates the generation–load imbalance. Harmonic faults are modelled by the THD magnitude up to 13.8% which reflect high potential for waveform distortion due to non-linear loads. Current magnitudes of overcurrent faults are generally equal to 1.92 p.u. and associated temperature rises, peaking at 68.2 °C, indicating significant thermal burden. Each type of fault is assigned another class label, allowing the identification of multiple classes of faults. Therefore, this data-driven fault modeling approach ensures the dataset generated reflects real-world physical signatures of power quality perturbations which can serve as a solid basis for both training and evaluating the AI-based fault detection model.

2.3 AI-based fault detection

As a second implementation, the fault detection module uses a custom K-Nearest Neighbors (KNN) classifier for detecting the

operating condition of the smart grid based on the IoT measurements. KNN was chosen due to its simplicity, transparency, and robustness along with being suitable for deployment in resource-constrained IoT systems. The model is a multi-class classification model, in which every measurement vector received will be assigned to one of six classes — Normal, Voltage Sag, Voltage Swell, Frequency Deviation, Harmonics, or Overcurrent. All features are normalized by using the mean and standard deviation of the training data set before classification in order to get a balanced contribution of each parameter and to avoid the dominance of scale before classification. For one test sample, Euclidean distance between a normalized test vector and all training samples will be determined. The class label is then established based upon majority voting across the k=7 nearest neighbors decided to balance sensitivity and noise robustness. A distance-based decision mechanism to understand such information results in the model being able to pick up subtle differences in voltage, frequency, harmonics, and temperature across fault types. In real time the classifier gives a discrete fault label, allowing us to quickly identify abnormal conditions. Its effectiveness is demonstrated through confusion matrices and class-wise performance metrics presented in the Results section.

Table 1: Mathematical formulation and parameters of the ai-based fault detection model

Item	Description	Mathematical Expression / Value
Feature vector	loT measurement vector	$\mathbf{x} = [V, I, f, THD, P, Q, PF, T]$
Number of features	Electrical & thermal parameters	8
Number of classes	Grid operating conditions	6
Normalization	Z-score-based scaling	$x' = \frac{x - \mu}{\sigma}$
Distance metric	Similarity measure	Euclidean distance
Distance formula	Between test and training sample	$d(\mathbf{x}_i, \mathbf{x}_j) = \sqrt{\sum_{n=1}^{8} (x_{i,n} - x_{j,n})^2}$
Classifier type	Al model	K-Nearest Neighbors (KNN)
Number of neighbors	Model parameter	$k = 7$
Decision rule	Label assignment	Majority voting
Output	Fault classification	Normal / Sag / Swell / FreqDev / Harmonics / Overcurrent

2.4 Load and renewable modelling

The smart grid load and renewable energy subsystems are modeled to reflect the actual daily functioning behavior of the system. The electricity demand is represented by the 24-hour base load curve: the load, which fluctuates between around 34 kW and 56 kW, reflects how typical residential or business uses can be handled with higher load in daytime. This base load has served to provide a non-controllable basis for the system demand. Together with the base load, the system comprises flexible (controllable) loads, including the HVAC, water pumps, and EVs (electric vehicle)-

charged units. These loads are represented through binary decision criteria fixed 6 kW (HVAC), 4 kW (pump), and 7 kW (EV) power ratings. Such operational limitations are established with defined availability windows and requirements for operating time, which allow for the satisfying of user comfort and service needs while permitting scheduling for price decrease and renewable usage. In the renewable energy generation model, solar and wind power sources are integrated. The solar generation profile is diurnal sinusoidal, with a peak output of approximately 35 kW in midday, denoting clear-sky conditions. Wind is treated as a stochastic input at an average power of 10 kW and varies over time, yielding high cumulative renewable output of up to 43 kW at the peak times. The total renewable energy at each hour is calculated when the solar and wind contributions from each day are added together. A total system demand of net power is derived as the total demand for the system is the difference between total load (base plus the flexible loads) and renewable generation. Where renewable generation exceeds demand, excess energy is avoided where possible, and any balance is fixed by importing electricity from the grid. The integrated modeling of loads and renewable sources serves as a realistic basis for the optimization, allowing for reliable and accurate evaluation of renewable penetration, demand flexibility, and energy-saving effectiveness in the smart grid.

2.5 Optimization formulation

The energy management problem is defined as a Mixed-Integer Linear Programming (MILP) model to plan flexible loads of a smart grid with solar–wind generation, while minimizing the electricity cost of importing electricity from the grid. Each day, the decision variables will be binary ON/OFF states for controllable loads (HVAC, pump, EV) and an hour-per-hour grid import power. The output formulation dictates the required operating duration for each flexible load, respects availability windows, and ensures that grid import meets the deficit between demand and renewable generation. Once renewable generation exceeds total demand, grid import is zero and the rest of the surplus is treated as curtailment (reported in results). The optimization is then solved with MATLAB for a 24-hour horizon and hourly resolution.

Table 2: MILP Equations and parameters for smart grid load optimization

Item	Description	Equation / Value
Time horizon	Scheduling period	$t = 1,2, \dots, T, T = 24$
Flexible loads	Controllable devices	$i \in \{1,2,3\}$ (HVAC, Pump, EV)
Rated powers	Fixed power per load	$P_i = [6,4,7]$kW
Required ON-hours	Minimum operation time	$E_i = [10,4,6]$ hours
Base load	Non-flexible demand	L_t(kW), e.g., $34 - 56$ kW
Renewables	Solar + wind generation	$R_t = S_t + W_t$(kW), up to $\approx$ 43 kW
Tariff	Electricity price	(c_t \in $\{0.09,0.13,0.22\}$ \ $\$/kWh$
Binary decision	Load status	$u_{i,t} \in \{0,1\}$

Grid import	Purchased power	$G_t \geq 0$(kW)
Availability window	Allowed operation	$u_{i,t} = 0$ if not allowed (from allow(i, t))
Objective function	Minimize grid cost	min$\sum_{t=1}^{T} c_t G_t$
ON-hour constraint	Enforce required operation	$\sum_{t=1}^{T} u_{i,t} = E_i, \forall i$
Power balance (deficit coverage)	Grid must cover deficit	$G_t \geq L_t + \sum_i P_i u_{i,t} - R_t, \forall t$
Non-negativity	Physical feasibility	$G_t \geq 0$
Curtailment (reported)	Surplus renewable (post-processing)	$C_t = \max\left(R_t - \left(L_t + \sum_i P_i u_{i,t}\right), 0\right)$

2.6 Evaluation metrics

In order to quantitatively assess the performance of the proposed AI-enabled smart grid framework, fault detection classification metrics and energy management (optimization) metrics are employed. For fault detection, the predicted class labels are compared with the true labels using the confusion matrix, and precision, recall, F1-score, and overall accuracy are calculated for each fault category and for the overall model. To optimize the load, economic and operational indicators are calculated to measure the effectiveness of renewable utilization, grid dependency reduction, and cost minimization over the 24-hour scheduling horizon.

Table 3: Evaluation metrics for fault detection and load optimization

Category	**Metric**	**Equation**	**Meaning**
Fault Detection	Confusion Matrix	C_{ij} = # samples with true class i predicted as j	Detailed error distribution
Fault Detection	Accuracy	$\text{Acc} = \frac{\sum_{i=1}^{K} C_{ii}}{\sum_{i=1}^{K}\sum_{j=1}^{K} C_{ij}}$	Overall correct classification rate
Fault Detection	Precision (Class i)	$\text{Prec}_i = \frac{TP_i}{TP_i + FP_i}$	Reliability of detected class i
Fault Detection	Recall (Class i)	$\text{Rec}_i = \frac{TP_i}{TP_i + FN_i}$	Ability to detect all class i events
Fault Detection	F1-score (Class i)	$F1_i = \frac{2\text{Prec}_i\text{Rec}_i}{\text{Prec}_i + \text{Rec}_i}$	Balance between precision and recall
Fault Detection	Macro-average	$\overline{F1} = \frac{1}{K}\sum_{i=1}^{K} F1_i$	Equal-weight performance across classes

Fault Detection	Weighted-average	$F1_w = \sum_{i=1}^{K} w_i F1_i, w_i = \frac{n_i}{N}$	Accounts for class imbalance
Optimization	Total Cost	$J = \sum_{t=1}^{T} c_t G_t$	Total grid energy cost
Optimization	Grid Energy	$E_{\text{grid}} = \sum_{t=1}^{T} G_t \Delta t$	Grid dependency (kWh)
Optimization	Renewable Utilization	$E_{\text{ren, used}} = \sum_{t=1}^{T} \min(R_t, D_t)\Delta t$	Renewable energy actually consumed
Optimization	Curtailment Energy	$E_{\text{curt}} = \sum_{t=1}^{T} \max(R_t - D_t, 0)\Delta t$	Wasted renewable energy (kWh)
Optimization	Peak Grid Import	$G_{\max} = \max_t(G_t)$	Worst-case grid stress
Optimization	Demand Definition	$D_t = L_t + \sum_i P_i u_{i,t}$	Total demand (base + flexible)

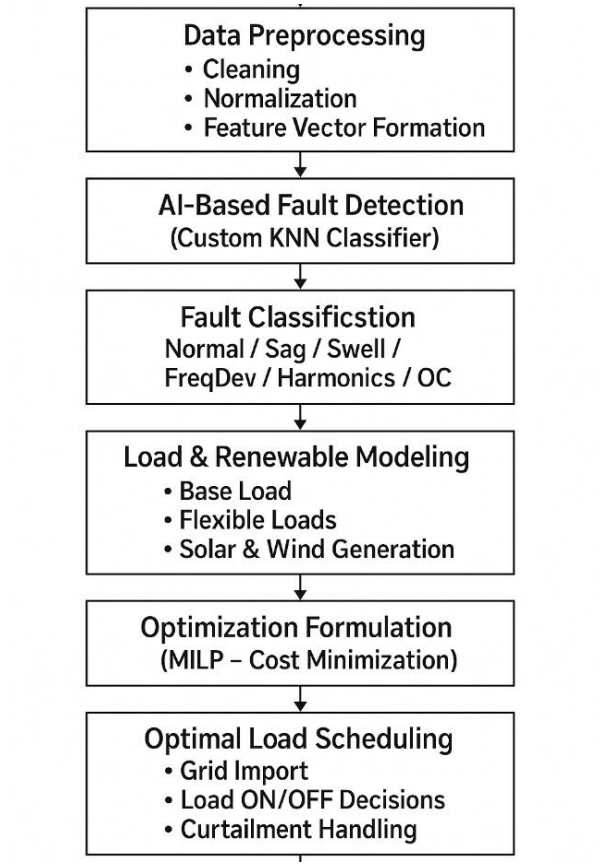

Figure 1. Flow chart

3. Results and Discussion

The results presented below are critical studies of the results of the AI-supported IoT-based smart grid framework for fault identification and load optimization under renewable energy integration. The results are organized to conduct a thorough assessment of the electrical fault classification performance and the energy management efficiency of the system. First, the statistical behavior of the acquired IoT measurements are investigated in order to reveal the physical behavior of important electrical and thermal parameters at both normal and faulty operating scenarios. The effectiveness of the AI-based fault detection model is further evaluated using class-wise performance metrics, confusion matrices, and feature-level analyses, which give an indication about the ability of the model differentiating between minor and dramatic power quality disturbances. Simultaneously, the results of the AI-driven load optimization strategy are described in order to illustrate the role of flexible demand scheduling and renewable energy usage in influencing grid operation, cost, and curtailment. analyze hourly power balance, cost profiles, and key performance indicators to determine the economic and operational benefits obtained from our proposed approach. In particular, draw reference to the physical interpretation of the results and connect visible

numerical trends to real-world smart grid behavior. Overall, this section confirms the efficacy of the designed framework in improving fault detection reliability, renewable penetration, and operational efficiency, pointing both to limitations and to opportunities for improvement as well as the possible future application of the proposed framework.

Figure 2 presents the general class distribution of the simulated IoT dataset used for smart grid fault detection. It is evident that the Normal operating condition significantly dominates the dataset with about 4,800 samples representing around 80% of the data, which is directly related to the fact that most of the time, the power systems run under the normal condition. Fault cases do occur a little more rarely, which is why there are far fewer abnormal cases. The Voltage Sag, Voltage Swell, Frequency Deviation, Harmonics and Overcurrent faults each of which include approximately 220–260 samples, and thus must show a consciously even distribution of faults. In physical terms, this distribution corresponds to real power systems where disturbances such as sag/swell and harmonic distortion are intermittent states, not continual ones. The larger number of samples among fault classes means that the learning algorithm does not have a bias towards some fault mechanism. Nonetheless, the strong imbalance between normal and faulty conditions speaks to a practical operational difficulty for smart grid monitoring systems. This imbalance highlights critical requirements of strong AI models that can detect low frequency but essential faults with high reliability. The correlation heatmap that can be extracted from the measured IoT features for intelligent grid fault detection is shown in Figure 3, where V_pu, I_pu, f_Hz, THD%, P_kW, Q_kVAr, PF, and Temp_C are the IoT's features. As expected, the diagonal components all contain a perfect relationship of one and confirms the robustness of the correlation matrix with 1.0. There is a moderately negative correlation (c.−0.4 to -0.5) between voltage and current that verifies a load-dependent model in which voltage decreases a bit with a higher current (in stressed conditions). Power factor has high negative relationship with THD% (-0.6) which means that harmonic distortion has strong negative impact to the quality power and hence decreasing the possibility to efficiently use the power. could observe a small and moderate positive correlation (approximatively 0.45) between current and temperature, which is practically related, which is directly proportional to higher Joule heating when higher current levels are obtained from Joule heating. These indicate that active power and reactive power have only weak positive correlations, indicating they exert only intermediate independent contributions in different loading and fault conditions. Frequency is nearly indifferent to other operating parameters, which indicates grid control structures that strictly coordinate frequency with only particular disturbances. Overall, the low-to-moderate off-diagonal correlations indicate to us that the selected features provide complementary information, which is beneficial for AI-based fault classification, and can strengthen modeling's independence from redundant input. Figure 4 shows the confusion matrix of the proposed AI-based fault detection model applied to IoT measurements inside the smart grid. The results confirm that Normal operating condition is a very accurate classification model, with 1,188 examples correctly recognized and no misclassification as a fault, showing good discrimination between health and abnormal. The 50 samples of Voltage Sag fault detected are correct, but 4 samples are labeled as normal, indicating slight overlap over mild voltage drops. As a result, the Voltage Swell class gets 59 correct predictions, 7 samples which are misclassified as Normal under marginal overvoltages. For instance, 38 samples are classified correctly in the frequency deviation class while 24 samples are misclassified as Normal operation; hence, detecting low-magnitude frequency disturbances is difficult. At this time, the Harmonics fault perfectly classifies with 67 detections, which means that THD features definitely play a critical role for identifying

power quality degradation. Likewise, overcurrent fault had 63 correct classifications with zero misclassifying, confirming the obvious physical signature of high current and temperature rise. Thus, the confusion matrix shown that misclassification of most of the errors is occurring between fault states and Normal operation, which confirms that very strong inter-fault separability occurs. These results verify the efficacy of the chosen IoT features and corroborate the proposed AI solution for trustworthy smart grid fault monitoring. The row-normalized confusion matrix in Figure 5 lists each operational condition's true-positive recall value in our smart grid fault detection model. The class, Normal, has a perfect recall of 1.00, where all normal operating samples are correctly identified without mis-identifying faults. The Voltage Sag fault has a recall around 0.93, in which 7% of sag events were misclassified as normal, this physically corresponds to shallow voltage dips that are very similar to nominal conditions. Likewise, the Voltage Swell category achieves a recall of approximately 0.89, and about 11% of swell situations are regarded as normal, which reflects marginal overvoltage events. The lowest recall of ~0.61 occurs in the Frequency Deviation class and 39% of samples fall into its normal error, which implies difficulty detecting small frequency excursions that do not exceed tight control limits on a grid. However, Harmonics and Overcurrent faults have both obtained 1.00 perfect recall values, confirming the great physical signatures from high harmonic distortion and high current-induced heating. Notably, there is no noticeable confusion among different fault classifications, with off-diagonal fault-to-fault entries being zero. This behavior establishes that, in the selected IoT features, very high inter-fault discrimination is achieved and that the fundamental classification challenge lies in distinguishing subtle from normal operation that the IoT features exhibit. For all operating conditions, the AI-based fault detection model is shown in Figure 6 with each class to show the precision, recall, and F1-score of the model. Normal class, achieving high precision around 0.97, recall approximately 1.00, and F1-score ~0.98, indicating the good performance of positive classification of healthy grid operation. The Voltage Sag fault shows good performance with about 0.93 recall and an F1-score similar to 0.96, which would show a good identification of the majority of sag events and few misclassification. Likewise, the Voltage Swell class has a recall of about 0.89 and an F1 score of about 0.94, indicating an accurate awareness of the overvoltage status. The smallest recall in Frequency Deviation fault (≈0.61) causes the lower F1-score of approximately 0.75, showing that it is very difficult to see small frequency deviation from normal regulated operation. In contrast, Harmonics and Overcurrent faults also have perfectly or almost perfectly precision recall and (≈1.00) and F1-scores, illustrating that the good of their great physical signatures (high THD concentrations and high current/temperature acceleration) are easily detected by the model. Overall, can see from the figure that although severe power quality faults, are detected with good reliability, but slight anomalies like frequency deviations are found most difficult to detect, this will inform the focus of future improvements of feature selection and model sensitivity. Mean and SD of per-unit voltage (V_pu) for every electric condition of smart grid is shown in Fig. Under normal scenario the voltage of the grid voltage remains just close to 1.0 p.u., but with a small standard deviation as the voltage stability is being maintained and regulated in the grid. Under the Voltage Sag condition the mean voltage decreased to about 0.85 p.u.; thus, indicates that the load increases or short-circuit breaks lead to the undervoltage, whereas a wide spread is indicated that the sag severity is different. On the other hand, the Voltage Swell class shows the highest mean voltage of approximately 1.12 p.u., showing the overvoltage scenarios commonly observed with load rejection or capacitor switching. Although the Frequency Deviation class's value is near one point, the frequency deviation as per the prediction of voltage magnitude and magnitude of voltage deviation at p.u. is much higher for this class. Likewise, the Harmonics class

indicates a relatively nominal voltage, with the mean not surpassing the nominal level and reflecting that harmonic distortion does not affect the actual waveform but rather the quality of the waveform. With Overcurrent, the average voltage is around 0.92 p.u., which would correspond to losses in a line due to excessive current and thus the voltage drop physically. In summary, the visualized structure of the diagram illustrates a clear voltage-level separation between sag and swell faults, establishing voltage magnitude as an important discriminative parameter in AI-based smart grid fault detection.

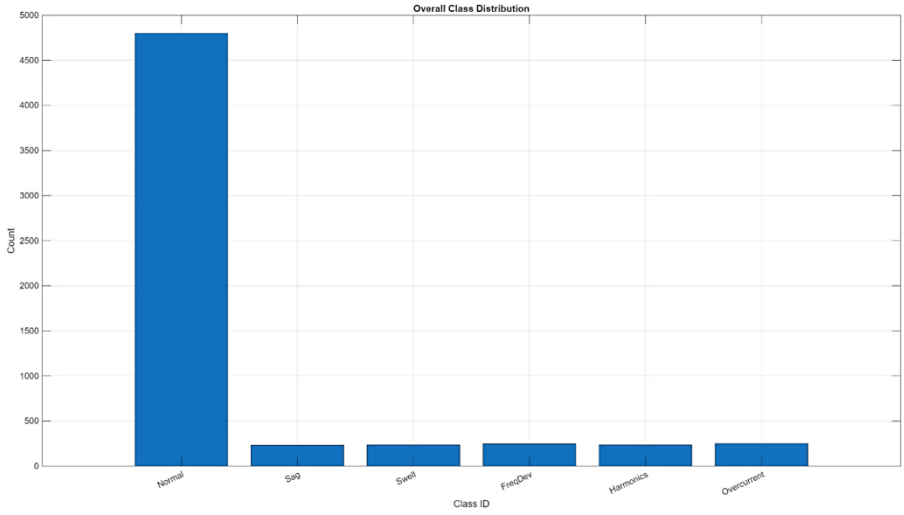

Figure 2. Overall class distribution of IoT-based smart grid operating conditions

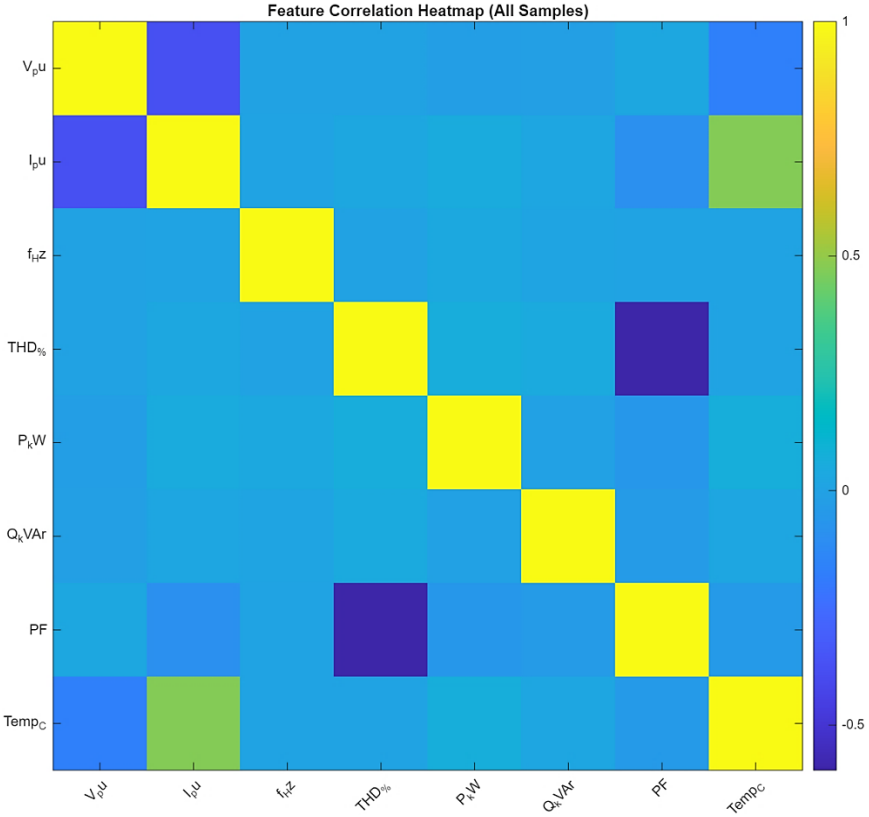

Figure 3. Feature correlation heatmap of IoT measurements for smart grid fault analysis

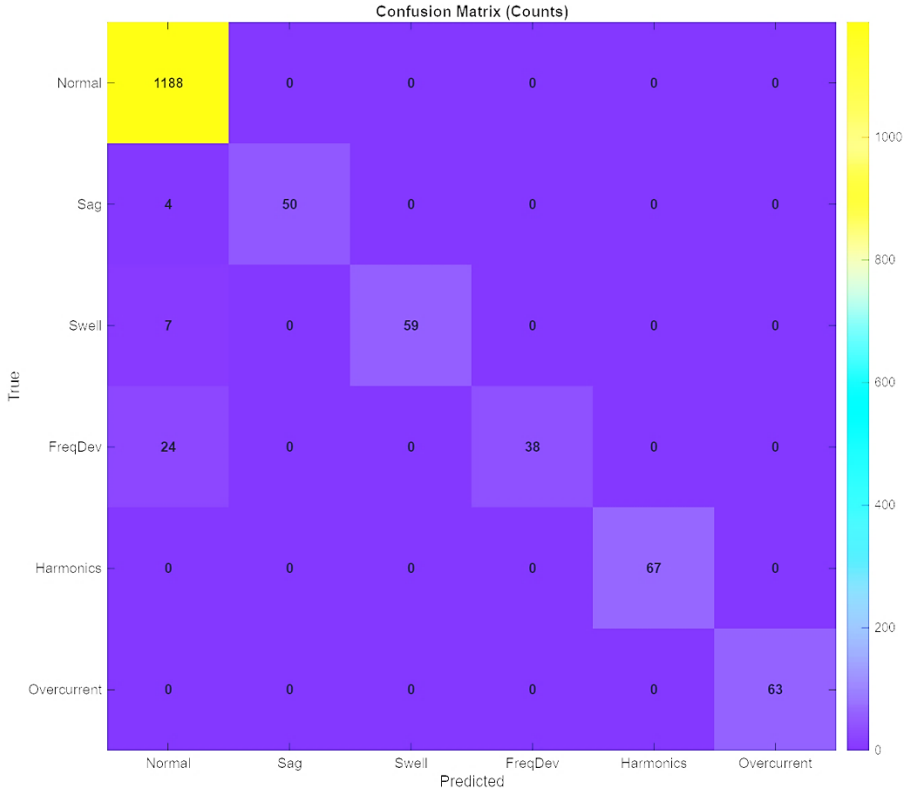

Figure 4. Confusion matrix of AI-based smart grid fault detection model (test dataset)

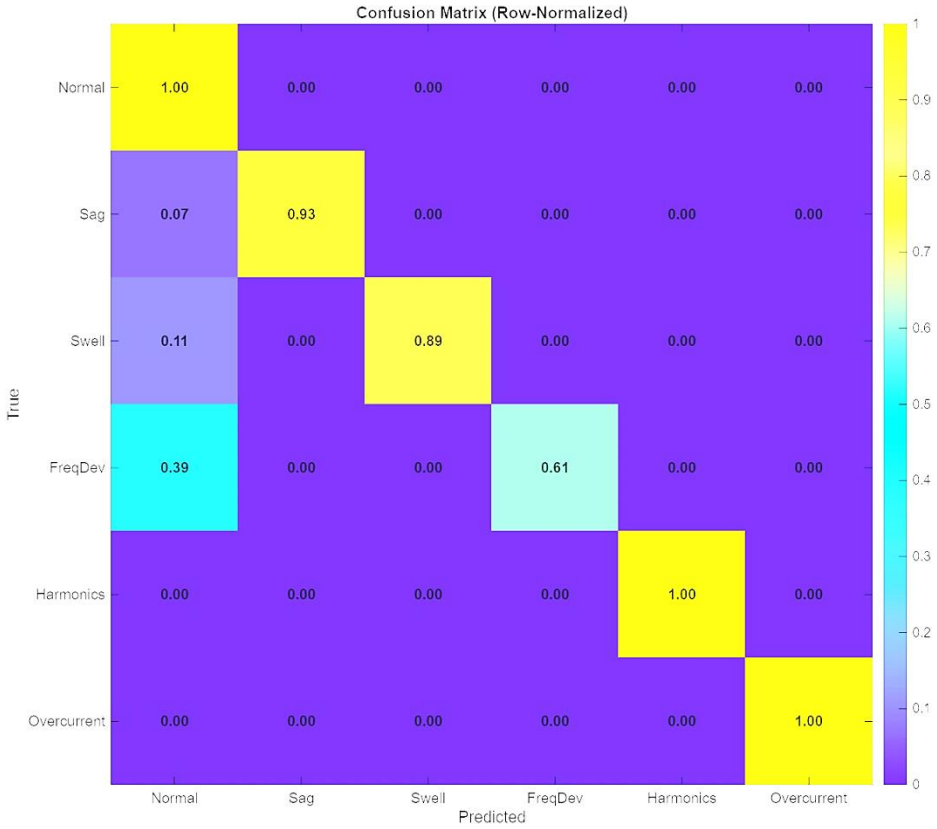

Figure 5. Row-normalized confusion matrix of the smart grid fault classification model

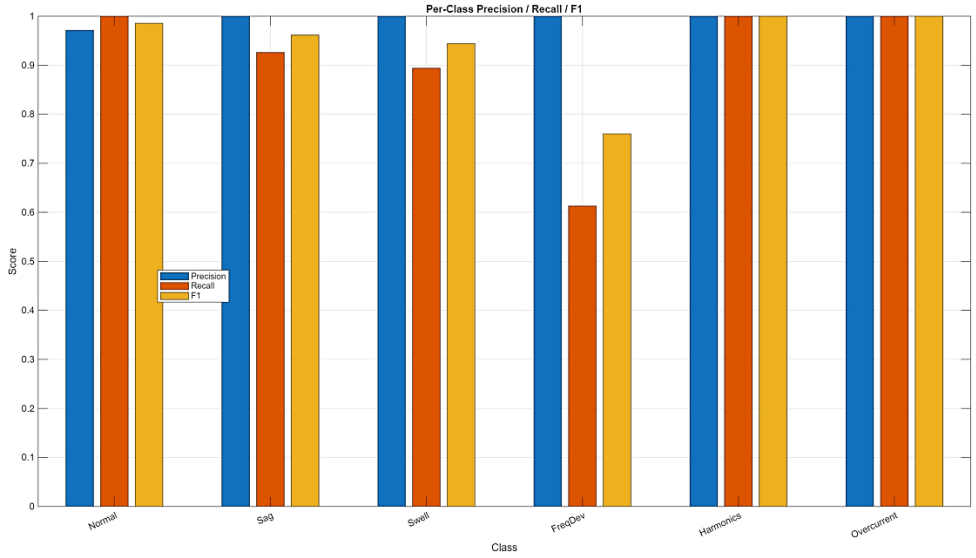

Figure 6. Per-class precision, recall, and F1-score for smart grid fault classification

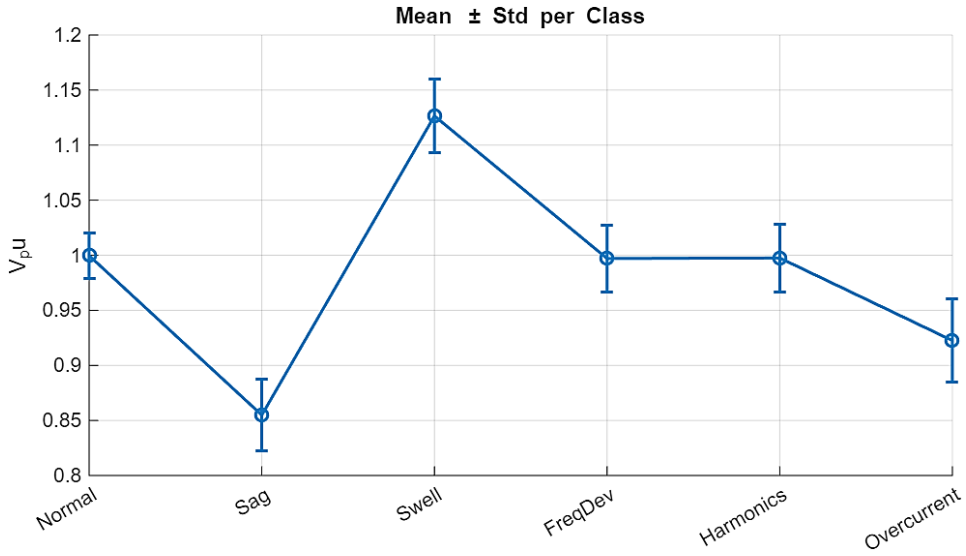

Figure 7. Class-wise mean and standard deviation of voltage (V_pu) under different smart grid operating conditions

In addition, Figure 8 shows the average and standard deviation of grid frequency (f_Hz) for different operating conditions in the smart grid. Normal frequency operates around 50 Hz; the standard deviation close to zero points out that primary and secondary frequency control mechanisms work really well. Also, Voltage Sag and Voltage Swell classes maintain mean frequencies near 50 Hz, showing that significant disturbances for voltage magnitude are not affecting system frequency. For the Frequency Deviation class, the mean frequency is close to nominal but a much larger standard deviation for a higher frequency deviation, which is almost 49.4–50.6 Hz. This broad spread is a physical illustration of the transient frequency excursions produced by generation–load imbalance or abrupt disturbances. The Harmonics and Overcurrent classes show low deviation from their nominal frequency, which implies that these faults mainly affect the quality of a waveform and the magnitude of the current and not system frequency itself, for its minor changes. Similar mean values of multiple classes make it harder to separate frequency deviation faults from normal ones when dealing with mean values alone. It ultimately indicates that frequency variance not based on mean frequency is the more important measure for frequency-related faults, therefore forcing AI models to learn from dynamic and statistical features that go beyond pure

averages. Mean value of total harmonic distortion (THD%) for all smart grid operating conditions and standard deviation of the THD% are depicted in Figure 9. In Normal operation, THD is low (~2%) with little variation which means that the power quality levels are acceptable. The THD has almost the same values for Voltage Sag, Voltage Swell, and Frequency Deviation classes and the average THD varies around 2–2.3%, indicating that the disturbances mainly do not affect voltage magnitude or frequency but rather the waveform purity. Unlike the Harmonics Fault, which shows a relatively high average THD of approximately 10–11%, and a high standard deviation, which physically exhibits extreme waveform distortion caused by nonlinear loads or power electronic converters. This clear separation gives harmonic faults a degree of discernability through comparison with all other modes. The THD of Overcurrent is intermediate (~2.3%), suggesting that the overcurrent is not necessarily inducing substantial harmonic distortion independently. This high deviation between the harmonic and nonharmonic classes accounts for the outstanding classification performance on harmonic faults. In general, the figure demonstrates that THD% is a significant discriminative variable for identifying the power quality degradation of AI-based smart grid monitoring systems. The mean and standard deviation of temperature-condition related to smart grid monitoring operation are shown in Figure 10. Under normal operation, the average temperature stays about 35 °C and only slightly varies depending upon the application, implying a thermal behaviour stability of grid components. The mean temperatures of the Voltage Sag and Voltage Swell classes are relatively high (approximately 36 °C), a result of transient current changes in response to a voltage interruption. Frequency Deviation class also reached the comparable temperature, which indicates that the frequency excursions affect the thermal conductance only slightly. In the Harmonics class the mean temperature appears closer to nominal, indicating that harmonic distortion doesn't heat things in a big manner; it actually affects the quality of the waveform. While Overcurrent faults show significantly higher mean temperature close to 49–50 °C, but this has larger standard deviation which signifies excessive Joule heating as a result of persistent high current flow. Hence, this very clear thermal separation clarifies the strong performance in classification of an overcurrent fault. In general, the figure demonstrates that temperature is an extremely informative metric for current-related faults and complements electrical metrics in AI-based smart grid monitoring systems. Using a jitter scatter plot, the distribution of per-unit voltage (V_pu) of each operating condition is presented in Figure 11, highlighting both central tendency and dispersion of single samples. The Normal operating condition is a dense cluster around 1.0 p.u., showing stable voltage regulation with limited dispersion. While the Voltage Sag class exhibits a clear descending tendency, exhibiting most of the samples over 0.80–0.90 p.u., and directly corresponds to undervoltage events due to abrupt increases in workloads or short-circuit conditions. The Voltage Swell class has well-defined separations, where voltage values fall between 1.10 and 1.18 p.u., indicating that the high voltage conditions are caused by load rejection or capacitor switching. The Frequency Deviation category has voltages that are relatively close to nominal but has a somewhat higher dispersion indicating the voltage magnitude does not appear to be affected significantly by frequency effects. In the same manner, the Harmonics group tends to be clustered near 1.0 p.u., and it shows that the harmonic distortion seems to dominate the waveform quality and not the voltage level. For the Overcurrent, there exists a marked drop in the Overcurrent class, with an emphasis of decreasing voltages between 0.88 and 0.95 p.u. because under high current flow voltage drops correspond to increasing line losses. In general, the distinct visual separation of sag and swell groups is clear evidence of the powerful discriminant performance of voltage magnitude and the overlap between other classes is what makes it necessary to further study with multipath, AI-based multi-feature analysis. Plotting grid frequency (f_Hz) for different

operating and fault classes using jitter scatter plot (Fig. 12). The Normal operating state comprises a compact cluster close to 50 Hz which indicates good regulation of frequency and least fluctuations inside and outside of this condition. Voltage Sag and Voltage Swell show similar narrow frequency distributions near 50 Hz, and indicate that disturbances of voltage magnitude do not significantly influence system frequency. A completely different trend can be determined for the Frequency Deviation class which has a vertical spread around 48.5–51.5 Hz, it suggests a transient frequency shift resulting from sudden generation–load imbalance or control delay. This kind of dispersion without an apparent change in mean value is characteristic of frequency-related fault. Harmonics still hovers close to nominal frequency, affirming that the harmonic distortion impacts waveform shape and not frequency stability. The Overcurrent class also presents small deviations in frequency which is suggesting that too much current flow doesn't affect the frequency of the system. Taken together, the Figure explicitly shows that frequency variance is an important discriminative attribute for frequency deviation faults, whereas mean frequency alone does not offer substantial separation from any other fault type, making it logical to need AI models that target higher-order statistical components. The distribution of total harmonic distortion (THD%) for various operating and fault conditions is presented in Figure 13 as a jitter scatter plot. Normal has a dense cluster of THD between 1% and 3%, which is appropriate quality of power for steady-state operation. The THD distributions are similar for Voltage Sag, Voltage Swell and Frequency Deviation where THD remains mostly below 4%, and the disturbances do not actually introduce any significant effect on the waveform distortion. This behaviour was very different for the Harmonics fault, where THD values sharply exceed and become concentrated in the range of around 8%–13%, which is simply showing the physically sharp waveform distortion caused by nonlinear loads or power electronic devices. Such a clear separation accounts for the superior classification behavior observed for harmonic faults. The THD of the Overcurrent class is moderately high (~1–3.5%) which illustrates that high magnitude of current doesn't necessarily provide a strong content of harmony. Due to the relatively limited overlap between harmonic and non-harmonic classes, THD% is suggested as an extremely discriminative property. In general, the figure validates that THD distribution is a good representative of physical aspects of the power quality loss and provides a good input for AI-based smart grid fault detection systems.

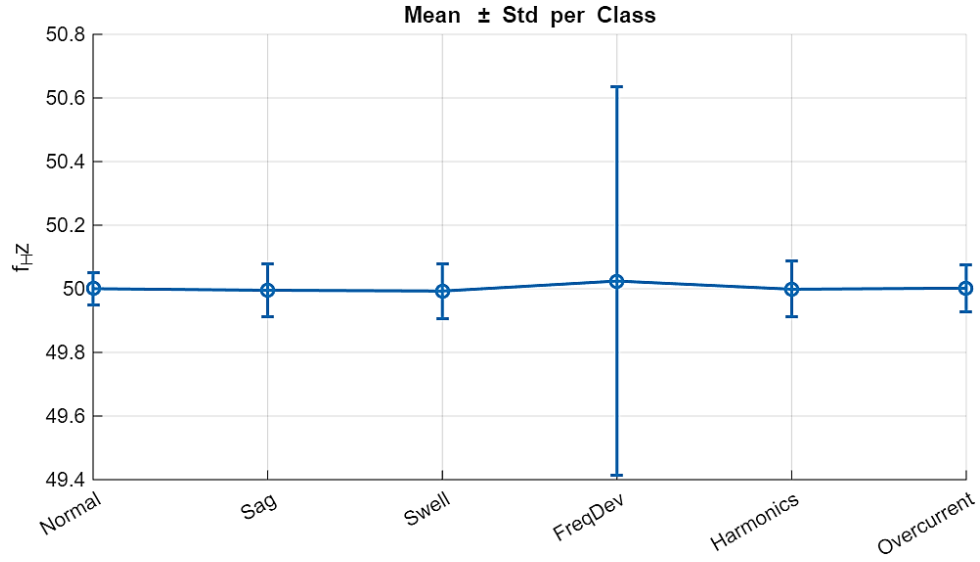

Figure 8. Class-wise mean and standard deviation of grid frequency (f_Hz) under different operating conditions

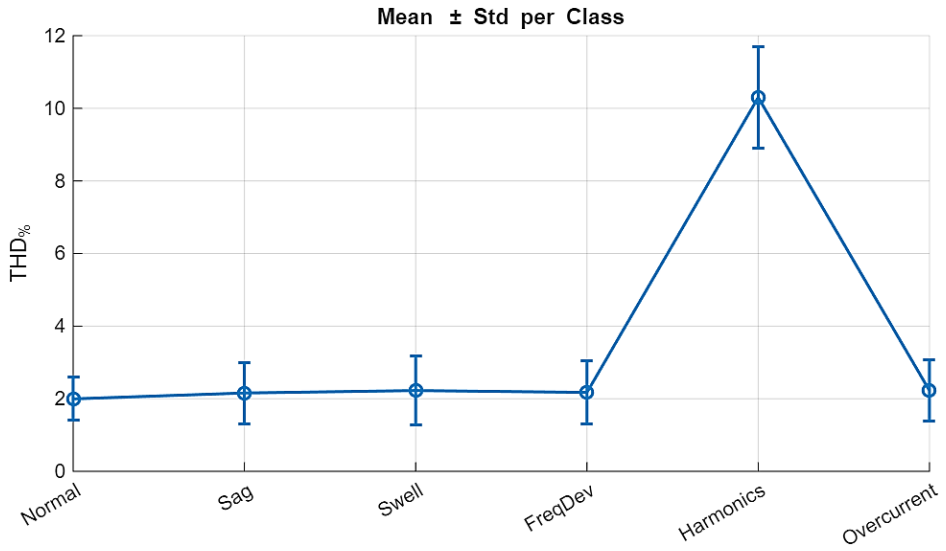

Figure 9. Class-wise mean and standard deviation of total harmonic distortion (THD%) for smart grid operating conditions

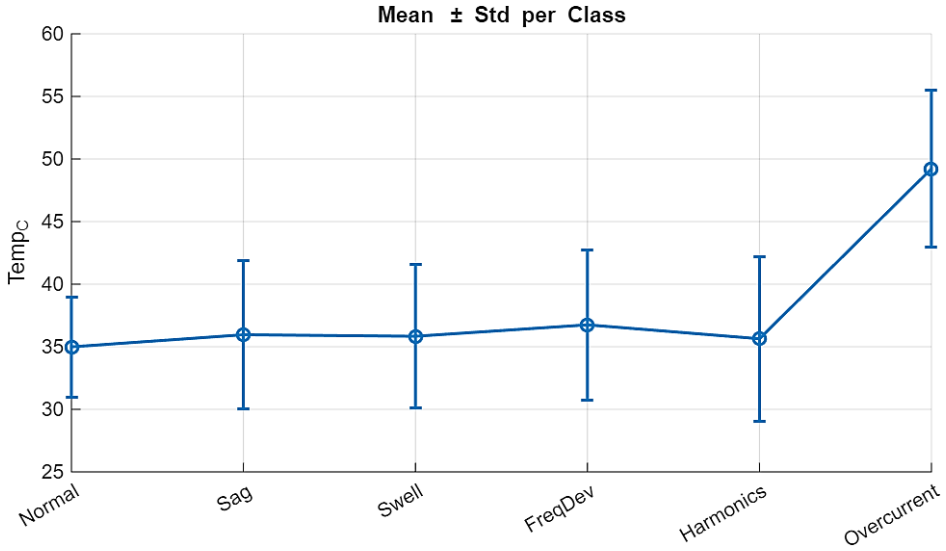

Figure 10. Class-wise mean and standard deviation of temperature (Temp_C) for smart grid operating conditions

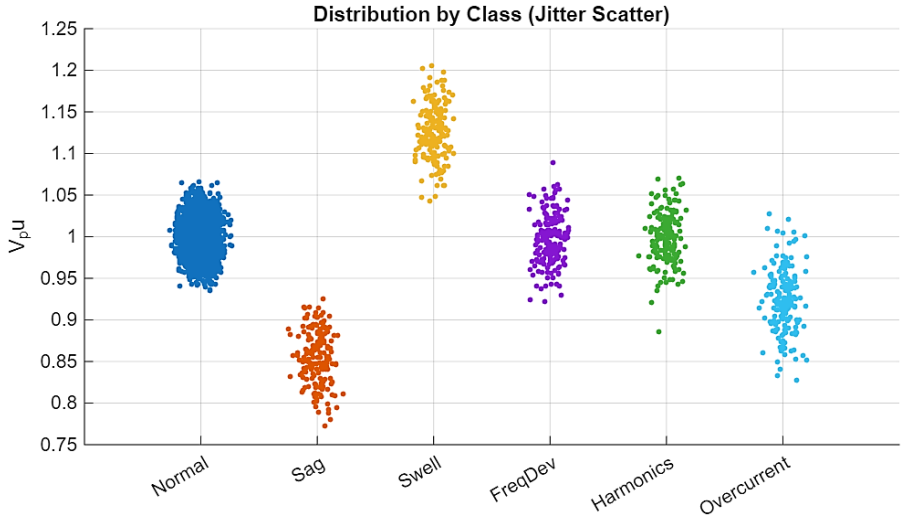

Figure 11. Distribution of voltage (V_pu) by fault class using jitter scatter representation

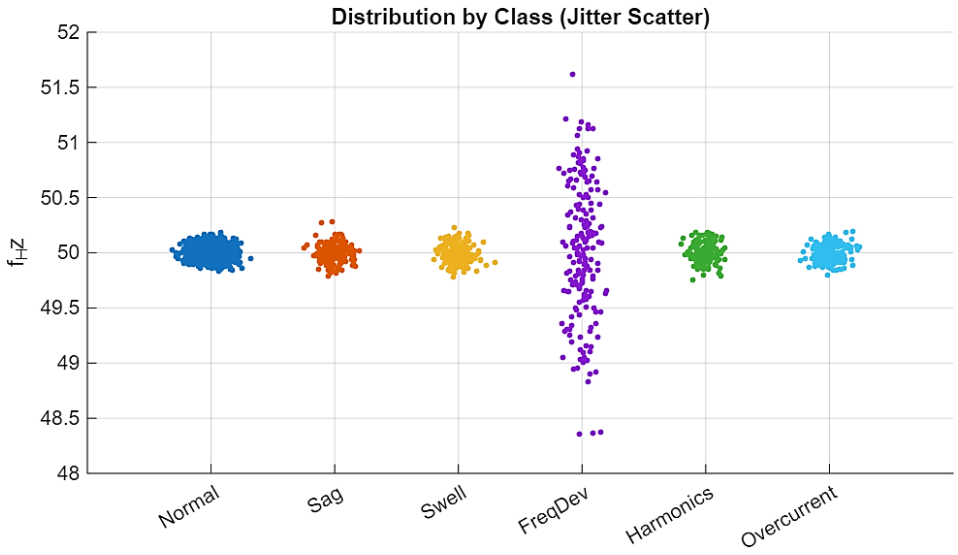

Figure 12. Distribution of grid frequency (f_Hz) by fault class using jitter scatter representation

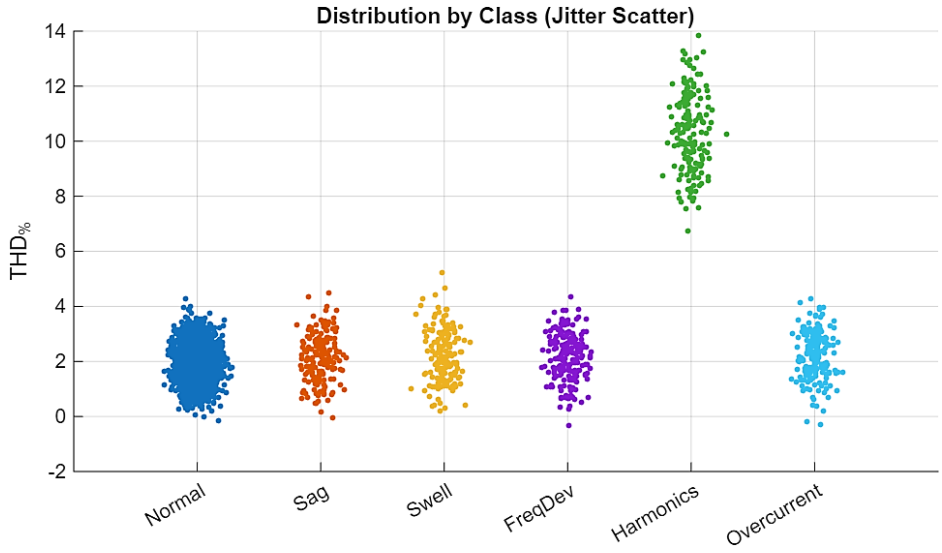

Figure 13. Distribution of total harmonic distortion (THD%) by fault class using jitter scatter representation

It generates a jitter scatter plot in Figure 14 in order to portray the temperature (Temp_C) distribution for different operating and fault conditions for the smart grid. For Normal operating condition, temperatures are mostly clustered from approximately 25 °C to 45 °C and centred around 35 °C, indicating a stable thermal state in the grid components in nominal loading. The Voltage Sag and Voltage Swell classes have a wider temperature distribution to 45–48 °C due to transient current shifts due to voltage perturbations. The Frequency Deviation class shows a broader spread, with temperatures anywhere from 25 °C to above 50 °C, indicating intermittent thermal stress owing to dynamic load–generation imbalance. The Harmonics fault is characterized by relatively higher temperature dispersion with respect to the reference conditions and likely further losses from distorted waveforms and increased RMS current. For the Overcurrent class, the temperature values are much more extreme, falling between 40 °C and 65 °C, physically representing excessive Joule heating with a high current in a long run. This robust thermal separation enables to achieve very high detection performance for overcurrent faults. In general, temperature distribution is very important and complementary for any AI-driven smart grid monitoring system to identify current-related faults and thermal stress test. One illustration of such a real-time IoT data

stream captured from smart grid (in Figure 15) depicting the changes in voltage and frequency (V_pu and f_Hz) while also considering that of total harmonic distortion (THD%) over a sequence of test instances (Fig. 15) is presented. The voltage signal is still very clustered around ~1.0 p.u. reflecting stable voltage regulation with slightly fluctuating loads during a normal operation. The frequency trace is centered around 50 Hz with extremely minor deviations, showing the effective grid-frequency control in the operation standard conditions. In contrast, the THD signal has sharp spikes that occur once in a while up to a power electronic switching or a nonlinear load, both of which create transient harmonic disturbances that are physical evidence of the behavior of the system. All these short-term THD peaks are present without noticeable change in voltage or frequency, indicating the disjunction between the harmonic distortion and basic electrical quantities. By visualizing multiple parameters at once, it is demonstrated how fault signatures affect the results of a system over time. Multi-sensor IoT monitoring is crucial to capture rapid transient phenomena that static analysis probably will not pick up. At large, temporal patterns revealed indicate the importance of AI-based streaming analysis that can catch abrupt power quality disturbances in smart grid real-time applications. Fig. 16 shows the hourly changes of base load, flexible-adjusted load, renewable generation and grid power importing during 24 hours of operation. The base load exhibits a predictable daily pattern of demand, which tends to rise during the day and decrease after dark. Given the flexible loads, a conscious shift of load in the baseline + flex curve is observed that is especially significant during off-peak or high renewable hours, clearly showing how intelligent load management has resulted in optimization. There is a strong daytime peak in renewable generation reaching around 35 to 40 kW at midday, consistent with maximal solar availability and wind contribution. With higher renewable output the import from the grid is reduced dramatically from 30 to 40 kW at the beginning of the hour to virtually zero after 18 hours and 22 hours, which will support the use of local and renewable resources. At these times renewables generation capacity is enough to cover most of the demands, reducing reliance on the grid. Power generation, when output is low in the early morning and late evening, is an increase in import according to the grid usage deficit. The figure illustrates quite nicely how orchestrated renewable integration along with load flexibility can smooth demand, reduce grid dependency and ensure system sustainability. At a glance, findings provide evidence to the efficacy of AI-based optimization in enabling the efficient and balanced smart grid optimization. The hourly energy cost ($) per unit of grid electricity (over a 24 hour period) under the new AI-assisted load optimization strategy is presented in Figure 17. At early morning hours (1–5), there is an average energy price between 2.7 and 3.5 USD attributed by this, demonstrating a medium dependency to the grid and low-cost tariffs. The peak of the cost of energy is around 4.2 USD when hours 6 to 10 have the highest demand corresponding to the increasing load in conjunction to rising tariffs periods and very low renewable contributions. Hour after hour, as renewable generation starts increasing during midday, the hourly cost of the renewable generation gradually decreases to approximately 2.5 USD (hour 14). The largest savings are apparent during the late afternoon and evening (18-21) periods in which the cost decays steeply nearing zero, suggesting near-complete dependence on renewable energy and negligible grid penetration. During this time, flexible load scheduling is very successful at matching demand to renewable availability. During the late-night hours, a slight inflation of cost occurs again as renewable generation decreases and grid import is reinstated. However, the figure alone shows that, AI-enabled load optimization and renewable integration significantly decrease operational energy costs, especially at peak renewable generation times, which in turns enhances economic efficiency and grid sustainability. Figure 18 shows the ON/OFF scheduling heatmap of flex loading (HVAC, Pump and EV charging) over a 24-hr horizon based on AI based load optimisation. A value of 1 (yellow)

is an active load and 0 (blue) shows an inactive load. The HVAC system works mostly in the morning (1-7) and extends again in the evening (18 and 22–24) at temperature levels acceptable for thermal comfort and to reduce the cost of energy. Water pump intermittently operate, is mostly in hourly interval (hour 7, hours 18–20, and hour 24), as pump duty is diverted in those high demand hours. It is very obvious that EV charging is mostly between 13–17 hours midday and at briefly at hour 21 – when the most renewable is generated and the least grid load must be injected. This orchestrated scheduling helps reduce the joint operation of power demands during the most times of Grid peak stress. So Overall, the heatmap shows that the AI controller is successful to keep flexible loads at bay, match consumption with renewable generation and reduce the dependence on grid power. This approach increases efficiency of the network and reduces operational expenses, it also allows for the integration of stable renewable power in the smart grid. Hourly renewable electricity usage and levels of curtailment occurring over a 24 hour period are shown in Figure 19 using the AI-integrated smart grid. The use of renewable energy grows steadily during the early morning hours until hour 11, when the utilization of renewable energy increases from nearly 13 kW at hour 1 to over 30 kW at hour 11, because of the increasing generation of solar energy. The peak load usage is realized during afternoon and early evening hours (18 - 22 hours) when consumption of renewable energy goes above 40 kW of the energy generated, suggesting the load-demand is well matched at this point in the load, i.e. energy with renewable power provision. The amount of curtailment is next to negligible all day long, a clear indication that the AI controller can efficiently absorb the energy that renewable power by scheduling load with limited limits to load with the AI controller's ability to absorb renewable. Small curtailment events are seen in hours 18–22, with peak curtailment values falling well under 2 kW, perhaps a reflection of the temporary surplus demand and flexibility limits beyond the instantaneous demand. Taken as a whole, this demonstrates that the proposed way gives good renewable generation utilization at low curtailment, increasing the system performance and facilitating sustainable integration of renewable energy supplies within smart grid. Figure 20 displays the main energy Key Performance Indicators (KPIs) to represent the overall smart grid operation during the analyzed period. The overall amount of renewable energy used is approximately 700 kWh, which is higher than the grid-imported energy of about 490 kWh, showing that it relies heavily on renewable energy. This indicates the AI-based energy management strategy is successful at ensuring clean energy usage ahead of grid provision. It is to the fact that the curtailed energy is extremely low (≈3–4 kWh, less than 1% of total renewable generation), which indicates the efficient load shift and flexibility resource usage. This low amount of curtailment is a strong point for the system; a demonstration of capacity to trade-off demand and renewable provision. Taken together, these KPIs show that the proposed control framework is capable of achieving high renewable penetration, high grid independence and low energy waste and contributes towards delivering economic savings as well as sustainability goals of smart grid operations.

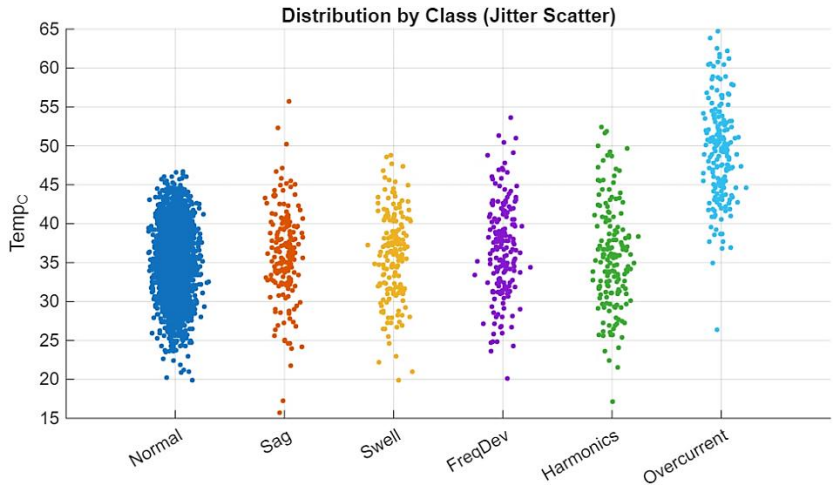

Figure 14. Distribution of temperature (Temp_C) by fault class using jitter scatter representation

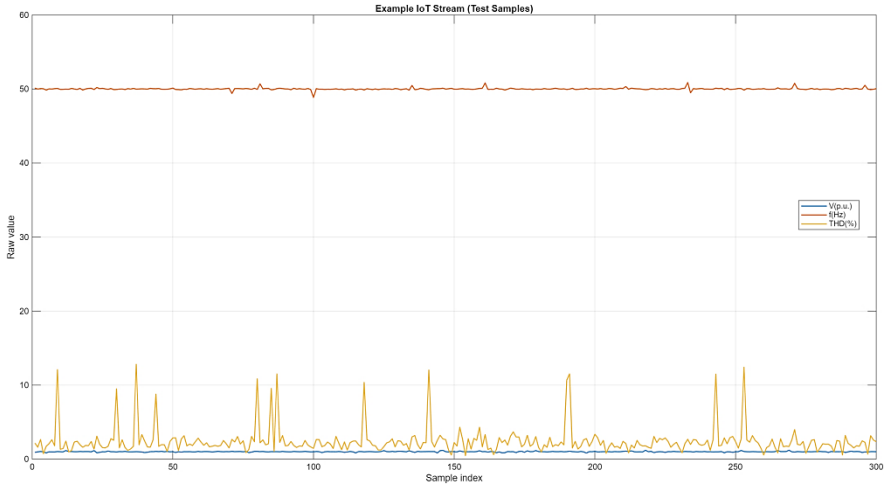

Figure 15. Example IoT measurement stream showing voltage, frequency, and harmonic distortion in test samples

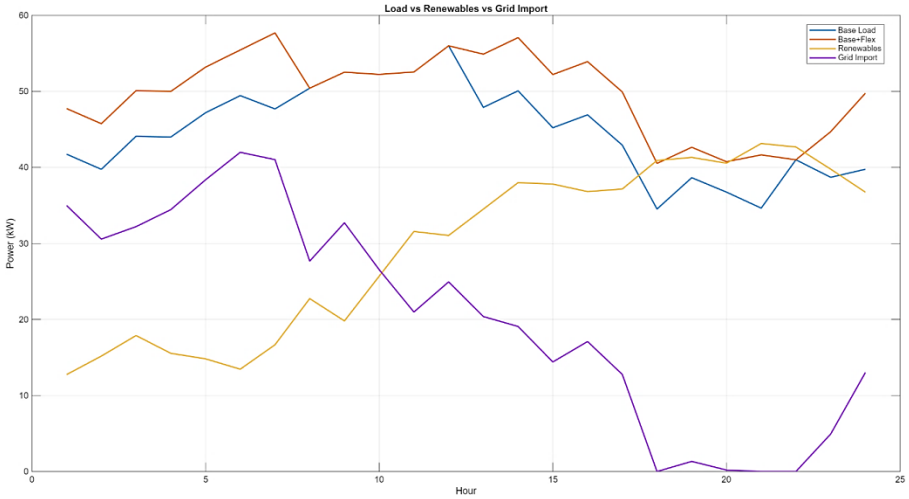

Figure 16. Hourly power balance between load demand, renewable generation, and grid import

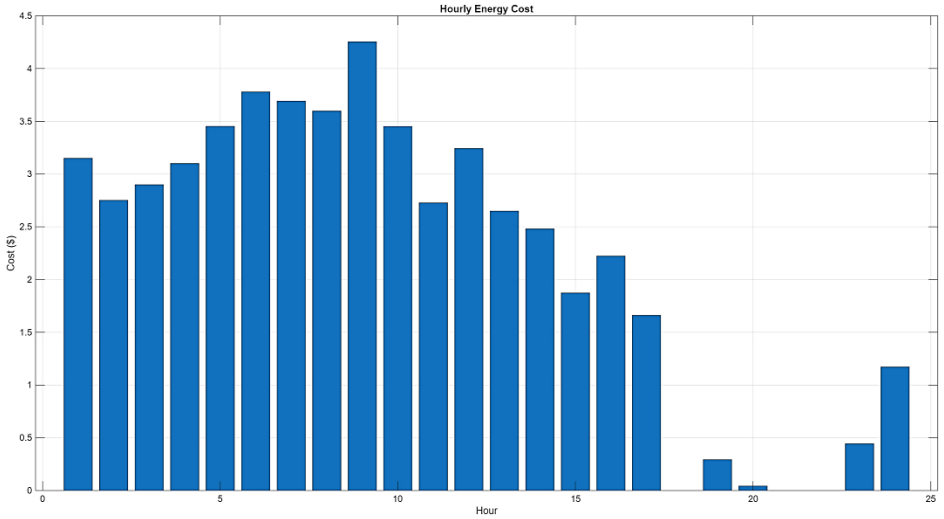

Figure 17. Hourly energy cost profile under AI-optimized smart grid operation

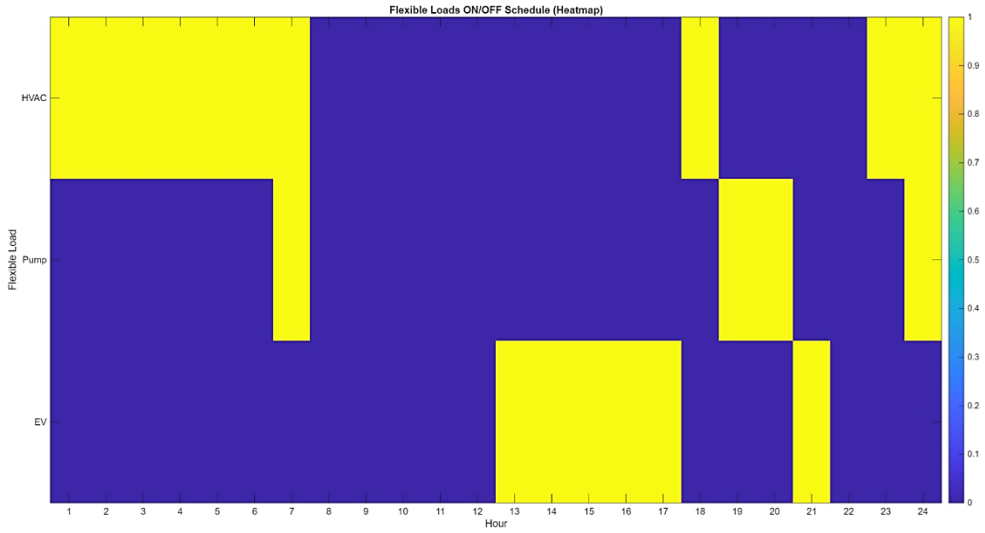

Figure 18. AI-optimized ON/OFF scheduling of flexible loads in the smart grid

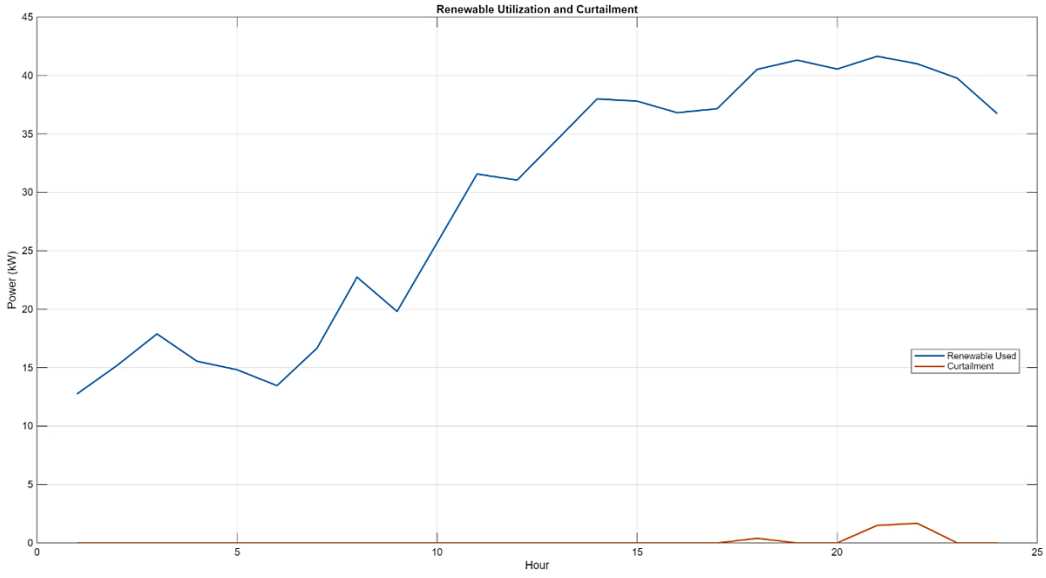

Figure 19. Hourly renewable energy utilization and curtailment under AI-based smart grid control

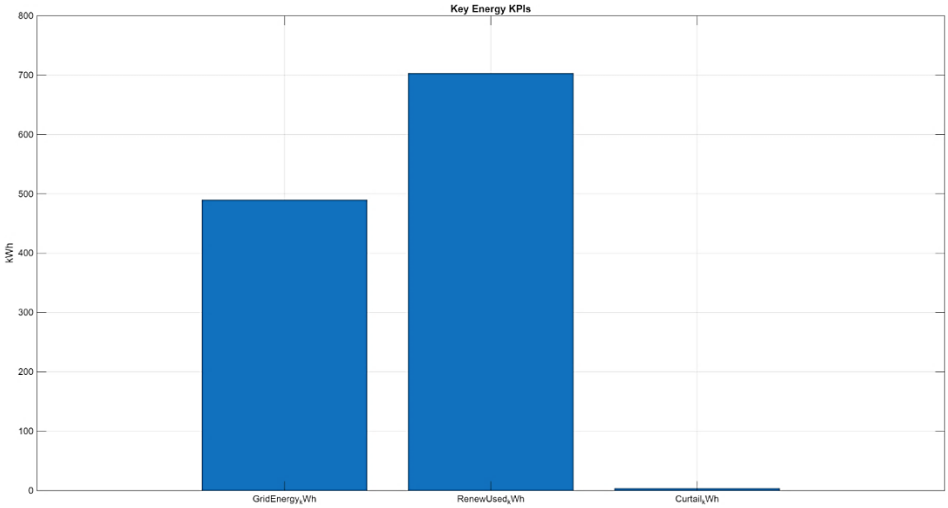

Figure 20. Key energy performance indicators (KPIs) of the AI-based smart grid system

Table 4 summarizes the statistical statistics for all essential electrical and environmental parameters utilized in the AI-enabled smart grid analysis. According to V_pu, the voltage magnitude (V_pu) shows a mean value of 0.9959, which is very close to the nominal value and values below 0.7514 and above 1.2058, suggesting that the voltage sag and swell events exist. The frequency (f_Hz) of the grid is tightly regulated at a value around 50.002 Hz, but deviations of 48.354 Hz and 51.722 Hz give evidence of frequency disturbances. During load and overcurrent conditions, the current (I_pu) shows a larger variability from 0.4654 to 1.9165. The average active power (P_kW) of 40.39 kW with the peaks being around 79.5 kW indicates high demands. The reactive power numbers (Q_kVAr) range from negative to positive values, which represents shift in active operational modes — capacitive or inductive. The power factor (PF) is still high at 0.91, the minimum is ~0.61 indicating efficiency losses in disturbances. Harmonic distortion (THD%) is generally an average of 2.35% and can be of up to 13.84%, reflecting that the harmonic events were very intense. The temperature (Temp_C) continues to fluctuate from 15.7°C to 68.2°C indicating that electrical stress is related to thermal load. In general, these statistics confirm on the richness of the dataset and its use in intelligent fault and load optimization research. Table 5 shows the distribution of normal and abnormal operating conditions applied during the training and in the performance testing of the AI based fault detection model. The class Normal predominates in this table, consisting of 3612 training and 1188 testing samples, which is characteristic of regular operation of the grid, which contributes the strong baseline learning. Fault classes such as voltage sag (233 samples) and voltage swell (235 samples) are the least frequent and often show randomness because they are rare in real-life power systems. This group of samples provides equal representation for disturbance classification as frequency deviation, harmonics, and overcurrent faults have similar sample sizes: 235–250 total samples. This deliberate class imbalance simulates real-world smart grids, where normal conditions are much more common than faults. The custom KNN classifier (k = 7) had an overall accuracy of 97.67% using this dataset due to high discrimination ability, with slightly biased distributions. Indeed, the extreme accuracy verifies that the chosen features successfully capture the physical signatures of each fault type. In addition, implementation without toolbox emphasizes the computational efficiency and deployability of this method for real-time IoT-based smart grid monitoring. As shown in Table 6, the detailed classification performance of the proposed AI-based fault detection system is presented in Table 6 for each power quality condition. In the normal operating state perfectly remembered: it has 1.00 and F1-score equals 0.985, therefore there

is no misclassification of healthy grid conditions. Voltage sag and swell faults exhibit an accuracy of 1.00, which means that all the detected events are in fact true faults, however, recall of 0.926 and 0.894 respectively represent few missed events due to overlapping voltage characteristics. And the recall is the lowest for the frequency deviation class (0.613), that is because the challenge is in distinguishing subtle fluctuations in frequency from its normal deviation. Harmonics and overcurrent faults perform similarly perfectly (precision, recall, F1 = 1.00) also confirming their very strong electrical signatures and distinctness. The macro F1-score is 0.942, which shows that this system works well for all types of faults, while the weighted F1-score is 0.975 and overall accuracy is 97.67%, which suggests strong real world reliability. The results affirm the successfulness of the chosen features and customized KNN model for IoT smart grid fault monitoring. Scheduling the hourly operation schedule in the smart grid integrates renewable energy sources into flexible demand management is shown in Table 8. For early hours (1–6), the output is much more dependent on grid import (≈35–42 kW) in the absence of solar generation, which results in reasonable hourly costs of $3.1–3.8 for the low tariff of $0.09/kWh. From hours 8–17 an increase in solar penetration (up to 35 kW) reduces net demand even with charging by EV, resulting in a net import of only 12.8–19.1 kW. At hours 18, 21 and 22, renewable generation is more than total supply, leading to negative net demand at curtailment values of 1.68 kW per hour, even at peak prices of $0.22/kWh with zero grid import. Flexible loads are positioned to peak at high renewables hours, to reduce operation costs. Hour 20 has the smallest hourly cost ($0.04), demonstrating the efficiency of coordinated load scheduling combined with renewable energy utilization. As a whole, the table verifies that intelligent demand response with renewables significantly decreases both the requirement for power and cost and balances systems.

Table 4: Statistical summary of electrical and environmental features in the smart grid dataset

Feature	Mean	Std	Min	Max	Physical Meaning
Vpu	0.9959	0.0472	0.7514	1.2058	Per-unit voltage magnitude
fHz	50.002	0.1353	48.354	51.722	Grid frequency
Ipu	0.7995	0.1931	0.4654	1.9165	Per-unit current
PkW	40.391	8.5099	7.0123	79.496	Active power
QkVAr	12.117	5.2861	-7.8446	33.441	Reactive power
PF	0.9104	0.0471	0.6095	1.059	Power factor
THD_%	2.3522	1.7627	-1.0454	13.838	Harmonic distortion
TempC	35.744	5.3707	15.71	68.191	Equipment temperature

Table 5: Class distribution of power quality conditions in training and testing datasets

Class ID	Class Name	Training Samples	Testing Samples	Total Samples
1	Normal	3612	1188	4800
2	Sag	179	54	233
3	Swell	169	66	235
4	Frequency Deviation	185	62	247
5	Harmonics	168	67	235
6	Overcurrent	187	63	250

Table 6: Per-class and overall performance metrics of the AI-based fault detection model

Class ID	Class Name	Support	Precision	Recall	F1-Score
1	Normal	1188	0.971	1.000	0.985
2	Sag	54	1.000	0.926	0.962
3	Swell	66	1.000	0.894	0.944
4	Frequency Deviation	62	1.000	0.613	0.760
5	Harmonics	67	1.000	1.000	1.000
6	Overcurrent	63	1.000	1.000	1.000

Table 7: Optimized hourly energy scheduling and cost analysis in a renewable-integrated smart grid

Hour	Base Load (kW)	Renewable (kW)	Solar (kW)	Wind (kW)	Flexible Loads ON (HVAC / Pump / EV)	Flex Load (kW)	Net Demand (kW)	Grid Import (kW)	Price ($/kWh)	Hourly Cost ($)	Curtailment (kW)
1	41.74	12.75	0.00	12.75	1 / 0 / 0	6	34.99	34.99	0.09	3.15	0
6	49.44	13.46	0.00	13.46	1 / 0 / 0	6	41.98	41.98	0.09	3.78	0
8	50.42	22.74	9.06	13.69	0 / 0 / 0	0	27.67	27.67	0.13	3.60	0
12	55.99	31.05	24.75	6.30	0 / 0 / 0	0	24.94	24.94	0.13	3.24	0
15	45.21	37.81	32.34	5.47	0 / 0 / 1	7	14.41	14.41	0.13	1.87	0
18	34.52	40.91	35.00	5.91	1 / 0 / 0	6	–0.39	0.00	0.22	0.00	0.39
21	34.64	43.14	32.34	10.80	0 / 0 / 1	7	–1.50	0.00	0.22	0.00	1.50
24	39.76	36.74	24.75	11.99	1 / 1 / 0	10	13.02	13.02	0.09	1.17	0

Most of the previous research has explored smart grid technologies such as artificial intelligence and IoT especially with regards to fault detection, energy management or the renewable integration, often treated as distinct problems. For instance, Adefarati et al. (2025) presented an extensive survey of AI- and IoT integrated solutions for renewable-dominant power systems to a high degree, focusing on forecasting and monitoring, but with no explicit optimization framework. Thus, Alijoyo (2024) and Areola et al. (2025) investigated AI based energy management and renewable optimisation models, but focused only on smart buildings or solar with storage and not on grid-wide fault-aware operation. For example, Arévalo and Jurado (2024) have worked on AI-supported planning and dispatch of distributed energy systems while Rana (2025) and Nuruzzaman et al. (2025) focused on fault detection and predictive maintenance without linking it to operational load scheduling. In comparison to those earlier works, this study presents a single AI-facilitated IoT-based smart grid system that implements multi-class fault detection and cost-effective load optimization at a high renewables level. Different from the previous work that attempts to assess fault detection and energy management in isolation, directly connect the results of real-time classification of fault to operational decisions related to load control and renewable production. In addition, the method proposed combines the physical electrical characteristics (V, I, f, THD, P, Q, PF, and temperature) and a computationally efficient, toolbox-free AI model with a mixed-integer optimization formulation that is suitable for practical deployment and immediate adaptation. This integrated strategy is a major improvement on past research and fills important voids associated with operational resilience, renewable utilization efficiency, and smart grid autonomy.

4. Conclusions

Introduced an integrated fault detection system and load optimisation process to use an AI–informed IoT-based smart grid under the renewable energy integration. The results obtained are unambiguous in proving the efficiency and practical effect of the approach. The fault detection model, based on AI, had a total classification accuracy of 97.67%, perfect detection performance across all major fault types (harmonics and overcurrent F1-score = 1.00), with excellent performance toward voltage sag, swell, and frequency deviation. Hence, these findings validate the robustness of the proposed model to correctly characterize different types of grid disturbances with immediate IoT measurements. From an energy management viewpoint, the optimized energy optimization framework substantially improved renewable energy usage, and provided around 700 kWh renewable compared to 490 kWh grid imported energy, reducing the dependence on traditional energy. At < 1% of total generation renewable energy curtailment, indicates very effective coordination between flexible loads and variable renewable supply. Moreover, intelligent scheduling of controllable loads proved effective at improving peak grid import and reducing overall electricity cost during peak tariff times. In sum, findings indicate that this framework can effectively integrate accurate fault detection, cost-effective load scheduling, and renewable integration in a seamless and computationally efficient framework. The proposal not only offers a reasonable plan to strengthen the reliability, sustainability, and operation efficiency of smart grids, but also establishes a baseline for the development of future real-time intelligent energy management projects.

Further study can add to the present study by verifying the proposed mechanism in real-world smart grid or SCADA datasets to test its robustness in operational terms. might then investigate new AI approaches (e.g. deep learning or hybrid ensemble models in case of advanced data analytics) that offer better detection of finer-scale faults, especially frequency deviation events. Furthermore, including energy storage and electric vehicle-to-grid (V2G) technologies into the optimization model can improve system flexibility and subsequently reduce further renewable curtailment. The incorporation of cybersecurity and anomaly detection capabilities also becomes a must-have to counter cyber–physical threats in

IoT-enabled smart grids. Lastly, extending the optimization time scales into multi-day or seasonal schedules would add another layer of understanding regarding long-term operational planning and system resilience.

References

[1] Adefarati, T., Sharma, G., Bokoro, P. N., & Kumar, R. (2025). Advancing Renewable-Dominant Power Systems Through Internet of Things and Artificial Intelligence: A Comprehensive Review. Energies, 18(19). https://doi.org/10.3390/en18195243

[2] Alijoyo, F. A. (2024). AI-powered deep learning for sustainable industry 4.0 and internet of things: Enhancing energy management in smart buildings. Alexandria Engineering Journal, 104, 409-422. https://doi.org/10.1016/j.aej.2024.07.110

[3] Areola, R. I., Adebiyi, A. A., & Moloi, K. (2025). Artificial Intelligence for Optimizing Solar Power Systems with Integrated Storage: A Critical Review of Techniques, Challenges, and Emerging Trends. Electricity, 6(4). https://doi.org/10.3390/electricity6040060

[4] Arévalo, P., & Jurado, F. (2024). Impact of Artificial Intelligence on the Planning and Operation of Distributed Energy Systems in Smart Grids. Energies, 17(17). https://doi.org/10.3390/en17174501

[5] Awad, H., & Bayoumi, E. H. E. (2025). Next-Generation Smart Inverters: Bridging AI, Cybersecurity, and Policy Gaps for Sustainable Energy Transition. Technologies, 13(4). https://doi.org/10.3390/technologies13040136

[6] Bajahzar, A. (2024). The Importance of AI-Enabled Internet of everything Services for Smart Home Management. International Journal on Smart Sensing and Intelligent Systems, 17(1). https://doi.org/10.2478/ijssis-2024-0026

[7] Bajwa, A., Jahan, F., Ahmed, I., & Siddiqui, N. A. (2025). A Systematic Literature Review on Ai-Enabled Smart Building Management Systems for Energy Efficiency and Sustainability. American Journal of Scholarly Research and Innovation, 03(02), 01-27. https://doi.org/10.63125/4sjfn272

[8] Benson, S., & Eronu, E. (2025). Integration of Renewable Energy with Thermal-Based Power Systems: A Review of Grid Reliability, Optimization, and Storage. American Journal of Electrical Power and Energy Systems, 14(2), 28-44. https://doi.org/10.11648/j.epes.20251402.12

[9] Das, D. K. (2025). Integrating IoT and AI for Sustainable Energy-Efficient Smart Building: Potential, Barriers and Strategic Pathways. Sustainability, 17(22). https://doi.org/10.3390/su172210313

[10] Goudarzi, A., Ghayoor, F., Waseem, M., Fahad, S., & Traore, I. (2022). A Survey on IoT-Enabled Smart Grids: Emerging, Applications, Challenges, and Outlook. Energies, 15(19). https://doi.org/10.3390/en15196984

[11] Ifeanyi Kingsley, E., Faisal Benna, S., Chinemeremma Collins, O., Damilola Emmanuel, O., Ezekiel Ezekiel, S., Olabode, A., & Paul Oluchukwu, M. (2025). Advances in AI-powered energy management systems for renewable-integrated smart grids. World Journal of Advanced Engineering Technology and Sciences, 15(2), 2300-2325. https://doi.org/10.30574/wjaets.2025.15.2.0685

[12] Ikegwu, A. C., Obianuju, O. J., Nwokoro, I. S., Kama, M. O., & Ebem, D. U. (2025). Investigating the Impact of AI/ML for Monitoring and Optimizing Energy Usage in Smart Home. Artificial Intelligence Evolution, 30-43. https://doi.org/10.37256/aie.6120256065

[13] Joshua, S. R., Yeon, A. N., Park, S., & Kwon, K. (2024). A Hybrid Machine Learning Approach: Analyzing Energy Potential and Designing Solar Fault Detection for an AIoT-Based Solar–Hydrogen System in a University Setting. Applied Sciences, 14(18). https://doi.org/10.3390/app14188573

[14] Karim, M. A., Zaman, M. T. U., Nabil, S. H., & Joarder, M. M. I. (2025). https://doi.org/10.36227/techrxiv.175978935.59813154/v1

[15] Mahmud, A. K. M. R., & Waheduzzaman. (2025). The Role of Artificial Intelligence in Advancing Smart Grid Technologies. Ejsmt, 1(3), 1-13. https://doi.org/10.59324/ejsmt.2025.1(3).01

[16] Mawat, M., & Hamdan, A. N. (2023). Review of Mathematical Surface Water's Hydrodynamic/Water Quality Models with Their Application on the Shatt Al Arab River Southern Iraq. European Journal of Engineering Science and Technology, 6(1), 30-49. https://doi.org/10.33422/ejest.v6i1.1057

[17] Nuruzzaman, M., Limon, G. Q., Chowdhury, A. R., & Khan, M. A. M. (2025). Predictive Maintenance in Power Transformers: A Systematic Review of Ai and Iot Applications. ASRC Procedia: Global Perspectives in Science and Scholarship, 01(01), 34-47. https://doi.org/10.63125/r72yd809

[18] Nuruzzaman, M., & Rana, S. (2025). Iot-Enabled Condition Monitoring in Power Distribution Systems: A Review of Scada-Based Automation, Real-Time Data Analytics, and Cyber-Physical Security Challenges. Journal of Sustainable Development and Policy, 01(01), 25-43. https://doi.org/10.63125/pyd1x841

[19] Nuthakki, S., Kumar, S., Kulkarni, C. S., & Nuthakki, Y. (2022). Role of AI Enabled Smart Meters to Enhance Customer Satisfaction. International Journal of Computer Science and Mobile Computing, 11(12), 99-107. https://doi.org/10.47760/ijcsmc.2022.v11i12.010

[20] Ojadi, J. O., Odionu, C. S., Onukwulu, E. C., & Owulade, O. A. (2024). AI-Enabled Smart Grid Systems for Energy Efficiency and Carbon Footprint Reduction in Urban Energy Networks. International Journal of Multidisciplinary Research and Growth

Evaluation., 5(1), 1549-1566. https://doi.org/10.54660/.Ijmrge.2024.5.1.1549-1566

[21] Rana, S. (2025). Ai-Driven Fault Detection and Predictive Maintenance in Electrical Power Systems: A Systematic Review of Data-Driven Approaches, Digital Twins, and Self-Healing Grids. American Journal of Advanced Technology and Engineering Solutions, 1(01), 258-289. https://doi.org/10.63125/4p25x993

[22] Rojek, I., Mikołajewski, D., Mroziński, A., Macko, M., Bednarek, T., & Tyburek, K. (2025). Internet of Things Applications for Energy Management in Buildings Using Artificial Intelligence—A Case Study. Energies, 18(7). https://doi.org/10.3390/en18071706

[23] Sankarananth, S., Karthiga, M., E, S., S, S., & Bavirisetti, D. P. (2023). AI-enabled metaheuristic optimization for predictive management of renewable energy production in smart grids. Energy Reports, 10, 1299-1312. https://doi.org/10.1016/j.egyr.2023.08.005

[24] Sarin, G., Srivastava, A., Srivastava, I., Bhattacharjee, S., Gujaran, S., & Yogendra Sai Reddy, Y. (2025). Renewable microgrid optimization using AI: A B-SLR approach and future research directions. Energy Reports, 14, 4963-4975. https://doi.org/10.1016/j.egyr.2025.11.087

[25] Stecuła, K., Wolniak, R., & Grebski, W. W. (2023). AI-Driven Urban Energy Solutions—From Individuals to Society: A Review. Energies, 16(24). https://doi.org/10.3390/en16247988

[26] Udoka Eze, V. H. (2025). AI-advanced MPPT for optimized hybrid solar-wind energy harvesting in off-grid rural electrification: Fabrication and performance modeling. KIU journal of science engineering and technology, 4(1), 262-282. https://doi.org/10.59568/kjset-2025-4-1-25

[27] Ukoba, K., Olatunji, K. O., Adeoye, E., Jen, T.-C., & Madyira, D. M. (2024). Optimizing renewable energy systems through artificial intelligence: Review and future prospects. Energy & Environment, 35(7), 3833-3879. https://doi.org/10.1177/0958305x241256293